J Membrane Biol (2014) 247:231–238
DOI 10.1007/s00232-013-9627-7

# Distance Measurements and Conformational Analysis of *sn*-2-Arachidonoylglycerol-Membrane Sample by $^{2}H$–$^{31}P$ REDOR NMR

**Elvis K. Tiburu · Lingling Shen**

Received: 28 November 2013 / Accepted: 30 December 2013 / Published online: 9 January 2014


**Abstract** The purpose of these studies is to determine the intermolecular distances that define the location, orientation, and conformation of 2-AG in palmitoyl-oleoyl-phosphatidylcholine (POPC) lipid bilayers using rotational-echo double-resonance (REDOR) NMR. All five protons on the glycerol backbone of 2-AG were replaced with $^{2}H$ and the distance between the deuterons and naturally occurring $^{31}P$ on the POPC lipid headgroup determined with REDOR. To determine the distance from each deuteron to the phosphorus, the POPC headgroup was arranged in a hexagonal array. The 2-AG intercalates between the lipid molecules and the $^{2}H$ labels, resulting in an average distance of $z$ directly above or below the center of the parallelogram of the four phosphorus atoms $P_1$, $P_2$, $P_3$, and $P_4$. For different $z$ values, the $^{2}H$–$^{31}P$ inter-nuclear distances were 7.6–9.1 Å ($^{2}H$–$^{31}P_1$ and $^{2}H$–$^{31}P_{31}$) and 4.4–6.7 Å ($^{2}H$–$^{31}P_2$ and $^{2}H$–$^{31}P_4$). Each result involved the calculations and summation of 893,101 terms. Based on the curve-fitting parameters, the calculations with $z = 0$ fits the data the best, which means these methylene $^{2}H$ atoms are at the same level as the phosphate group of the POPC lipid bilayer. Molecular dynamic simulation data suggested that the $^{2}H$ atoms at the glycerol backbone of 2-AG are involved in an extended H-bonding network with the phosphorus atoms after 10-ns simulation.

**Keywords** NMR · Model membrane · Cannabinoid receptor · Endocannabinoids

E. K. Tiburu (✉)
Department of Biomedical Engineering, Faculty of Engineering, University of Ghana, Legon, Ghana
e-mail: etiburu@ug.edu.gh

E. K. Tiburu
Center for Drug Discovery, Northeastern University, Boston, MA 02115, USA

L. Shen
Department of Information Technology, Novartis Research and Development, Shanghai, China

## Introduction

Endocannabinoid (eCB) signaling is tightly controlled by phospholipid-derived neuroactive lipids such as *sn*-2-arachidonoylglycerol (2-AG) and *N*-arachidonoylethanolamine (anandamide) (Piomelli 2003; Di Marzo 2008; Murillo-Rodriguez et al. 2003). 2-AG is produced within lipid rafts utilizing 1,2-diacylglycerol (DAG) as a precursor molecule (Kozak et al. 2004; Szabo et al. 2006). As with typical neurotransmitters, the expression levels are low and transient with 2-AG rapidly deactivated after biosynthesis and release via cytosolic fatty acid amide hydrolase (FAAH) and monoacylglycerol lipase (MGL) (Cravatt et al. 1996; Dinh et al. 2002). Cannabinoid receptors-1 and 2 (CB1 and CB2) which are both resident in the central nervous system, and some parts of the periphery are targets of 2-AG, though the signaling properties on the CB1/2 receptors may also be an "entourage" effect originating from both 1-AG and 2-AG. This is feasible because acyl migration (non-enzymatic reaction) from the sterically hindered *sn*-2 position to the more stable *sn*-1 or *sn*-3 positions is a typical process for mono- and di-glycerides (Devane et al. 1992; Sugiura et al. 1995; Mechoulam et al. 1995; Matsuda et al. 1990). Indeed biochemical studies have been conducted that indicates 2-AG can be readily converted to 1-AG under conditions commonly used to study structure–activity relations, a limitation that impacts our understanding of the structural features of 2-AG and the mechanism by which it exerts its

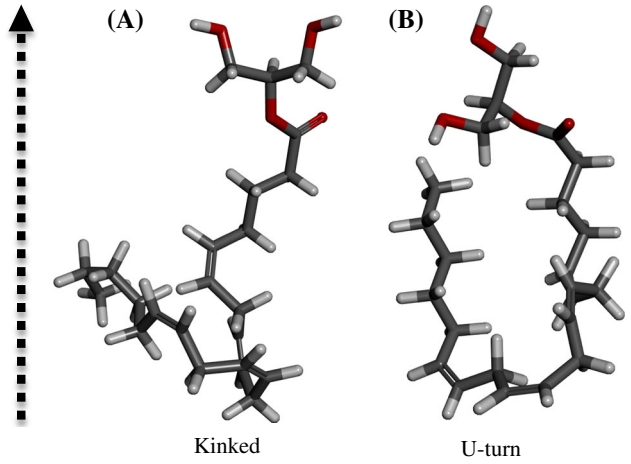


**Fig. 1** A 3D representation of 2-AG in membrane mimetic environment showing the 20-carbon chain on position two of the glycerol backbone. **a** Kinked, **b** curved conformations

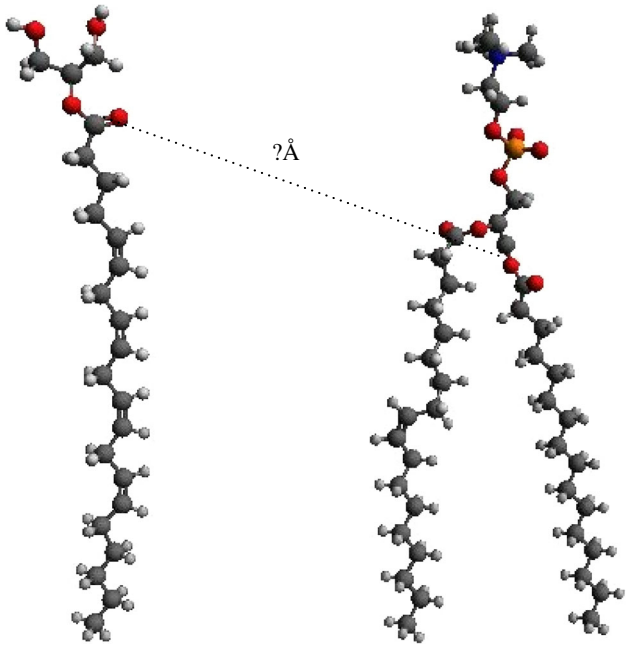


**Fig. 2** A cartoon depiction of the distance between 2-AG $^{2}$H on the *left*, and the phosphorus on POPC on the *right*. The $^{2}$H on 2-AG is shown with *gray color*, whereas phosphorus on POPC is depicted with *orange* (Color figure online)

psychoactive effects on membrane-bound proteins such as the CB1 or CB2 receptors.

From the above description of 2-AG, it seems the structural features of the molecule is defined by either its interaction with a transporter system, the membrane environment, the CB receptors and intracellular MGL and FAAH enzymes or all of the aforementioned scenarios. Because the precise membrane localization of 2-AG is crucial to its function, the geometrical description of the endocannabinoid must be identified and quantified without altering its spatial organization in the membrane. Currently, computational methods have been the major tools of research in the study of the mechanism of neurolipid/lipid interactions at the atomic level (Lynch and Reggio 2005; Hurst et al. 2010; Reggio 2010). It has been reported that 2-AG partitions into the bulk lipid and orient with its arachidonic tail in a kinked conformation and almost parallel to the long axis of the phospholipid bilayer (Fig. 1a) (Hurst et al. 2010). This conformation moves the terminal methyl closer to the center of the bilayer and in proximity to the phospholipid terminal $CH_3$ (Fig. 1a). The modeling data utilizing shorter simulation time frame, however, depict an U-turn conformation of 2-AG within the phospholipid bilayer, whereby the terminal methyl is directed toward the polar lipid headgroup (Fig. 1b). In the same studies, the glycerol moiety is stabilized by a preferred conformation through H-bonding network with water molecules and the lipid headgroup.

Other rigid-body small molecule drugs such as cholesterol, *Cannabis sativa* major active compound *delta*-9-tetrahydrocannabinol (delta 9-THC), have been studied in model membranes of DPPC and POPC utilizing $^{2}$H and $^{13}$C solid-state NMR (Tiburu et al. 2004; Tiburu et al. 2007; Guo et al. 2003; Mavromoustakos and Daliani 1999; Yang et al. 1992; Makriyannis et al. 1990). There is also evidence of the utilization of NMR methods to quantitatively extract orientational information from anandamide in model membranes, but such studies on the segmental mobility of 2-AG are yet to gain prominence (Tian et al. 2005).

The computational modeling data displayed in Fig. 1 invoke three questions about 2-AG; (1) the orientation of the glycerol moiety within the membrane environment and its structural preference, (2) the distance between key atoms within C(1) and C(3) on the glycerol moiety and the membrane headgroup/water interface, and (3) the location of the terminal methyl relative to the membrane center. Understanding the conformational dynamics and location within the cell membrane requires the measurement of inter-nuclear distances which would be highly significant to inform the nature of ligand/lipid interactions and may enhance our ability to design novel therapeutic medications to target the endocannabinoid system.

Rotational-echo double-resonance (REDOR) NMR is an established and powerful technique for measuring distances between two nuclei in the solid state (Goetz and Schaefer 1997). The technique takes advantage of the heteronuclear dipolar coupling between two different NMR-sensitive coupled spin pairs such as $^{2}$H and $^{31}$P. The dipolar coupling which depends on the inter-nuclear distance can be extracted for structural determination in solids. Our approach is to utilize POPC membrane preparation as a model environment to incorporate 2-AG and examine the geometric properties and the supramolecular organization between 2-AG and the lipid

molecules. This is accomplished by strategically identifying key atom pairs within 2-AG/POPC bilayer profile and incorporation $^{2}$H at specific sites on the 2-AG glycerol backbone and $^{31}$P at the phospholipid headgroup. The position of the labeling sites and proposed dipolar interaction between coupled spin pairs are shown in Fig. 2. The inter-nuclear distance is then determined using the REDOR techniques. REDOR uniquely allows the measurement of accurate distances between nuclei to about 8 Å and has been applied effectively to study small molecule drugs interacting with membrane proteins. Of note, this is the first direct approach to determine the binding conformation of a non-rigid-body drug such as 2-AG in model membranes of POPC with the REDOR technique and may reveal the mechanism of lipid-mediated signaling in the membrane.

## Materials and Methods

2-AG was synthesized to incorporate $^{2}$H at the glycerol site on carbon position C1, C2, and C3. For the NMR samples, aliquots of 2-AG were introduced into POPC lipids in chloroform to give a lipid/ligand molar ratio of 50:1. (Tiburu et al. 2004; Tian et al. 2005; De Angelis and Opella 2007). The resulting mixture was dried under a stream of nitrogen gas until the chloroform was completely evaporated and the dried sample was further allowed to sit in a vacuum overnight. The sample was hydrated with an HEPES buffer made from deuterium-depleted water to give a 70 % (w/w) POPC phospholipids to solution.

## NMR Spectroscopy

The $^{2}$H–$^{31}$P REDOR experiments were performed on a 16.4 T (700 MHz $^{1}$H Larmor frequency) magnet with MAS triple resonance (HXY) probe (Goetz and Schaefer 1997; Grage et al. 2004). The $^{1}$H $\pi/2$ pulse was set at 5 μs, and the $^{31}$P and $^{2}$H p pulses were 10 and 7 μs, respectively. The $^{1}$H and $^{31}$P cross-polarization (CP) time was 2 ms. $^{1}$H decoupling was set at 100–120 kHz during evolution and 80 kHz during acquisition (Tiburu et al. 2004, 2007; Guo et al. 2003). The pulse sequence employed was XY8-REDOR (Mavromoustakos and Daliani 1999), following the generation of solid-state NMR experiments at −68 °C on a 700 MHz Bruker AVANCE II NMR spectrometer using a 5 mm double-resonance probe under static sample conditions.

## REDOR Calculations

Geometry was based on an earlier paper on anadamide/phospholipids interactions and the structure of the Lc' phase in a hydrated lipid multilamellar system (Tian et al. 2005; Raghunathan and Katsaras 1995). The REDOR analysis is derived from previous work (Goetz and Schaefer 1997; Grage et al. 2004). The calculation involves a three-dimensional integral to simulate the "power sample" (Raghunathan and Katsaras 1995):

$$\frac{S}{S_0} = \frac{1}{8\pi^2} \int_{\psi=0}^{2\pi} \int_{\theta=0}^{\pi} \int_{\phi=0}^{2\pi} \prod_i \cos\left[4\sqrt{2}\tau D_i(\hat{n}'(i)\cdot\hat{y})(\hat{n}'(i)\cdot\hat{z})\right] \mathrm{d}\phi \, \sin\theta \, \mathrm{d}\theta \, \mathrm{d}\psi \quad (1)$$

where $D_i$ is the dipolar coupling constant of $i$ th $^{2}$H–$^{31}$P dipole pair ($i = 1, 2, 3, 4$),

$$D_i = \frac{\mu_0}{4\pi} \frac{h\gamma_P\gamma_D}{4\pi^2 r_i^3}. \quad (2)$$

Inter-nuclear distances:

$$r_1 = r_3 = \sqrt{z^2 + (b\cos 30^\circ)^2} \quad (3)$$

$$r_2 = r_4 = \sqrt{z^2 + (b\sin 30^\circ)^2} \quad (4)$$

The phase factors ($i = 1, 2, 3, 4$)

$$(\hat{n}'(i)\cdot\hat{z}) = [\sin\theta\cos\phi]x_i + [\sin\theta\sin\phi]y_i + [\cos\theta]z_i \quad (5)$$

$$\left(\hat{n}'(i)\cdot\hat{y}\right) = [-\cos\psi\sin\phi - \cos\theta\cos\phi\sin\psi]x_i + [\cos\psi\cos\phi - \cos\theta\sin\phi\sin\psi]y_i + [\sin\psi\sin\theta]z_i. \quad (6)$$

In our particular case,

$$x_1 = b\cos 30^\circ, \quad y_1 = 0, \quad z_1 = z \quad (7)$$

$$x_2 = 0, \quad y_2 = b\sin 30^\circ, \quad z_2 = z \quad (8)$$

$$x_3 = -b\cos 30^\circ, \quad y_3 = 0, \quad z_3 = z \quad (9)$$

$$x_4 = 0, \quad y_4 = -b\sin 30^\circ, \quad z_4 = z. \quad (10)$$

The constants in Eq. (2) areGyromagnetic ratio for $^{31}$P: $\gamma_P = 108.291 \times 10^6 \mathrm{rad/s/T}$,Gyromagnetic ratio for $^{2}$H: $\gamma_D = 41.065 \times 10^6 \mathrm{rad/s/T}$.Planck constant $h = 6.626068 \times 10^{-34} \mathrm{m^2\,kg/s}$.

$\mu_0/4\pi = 1.00 \times 10^{-7} \mathrm{T\ m/A}$.

The integral (Eq. 1) was carried out numerically using the Simpson method with angular increments of $\pi/60$ for $z = 0, 1, 2, 3$ Å, etc.

## Computational Methods

Both 10-ns simulations of 2-AG were undertaken using the Desmond molecular dynamics software package with an

OPLS-AA 2005 force field including data for the POPC bilayer, along with the SPC model for water (Bowers et al. 2006; Jorgensen et al. 1996). Force field parameters for 2-AG were constructed by utilizing existing parameters for similar atom types. In the simulation setup, M-SHAKE constraints were used on all covalent bonds involving hydrogen atoms to allow an iteration time step of 2 fs (Kräutler et al. 2001). The reference system propagator algorithm (RESPA) was used to integrate the equations of motion using periodic boundary conditions on this orthorhombic simulation system (35 Å × 30 Å × 20 Å) (Tuckerman et al. 1991). Constant pressure was maintained using the Martyna–Tobias–Klein (MTK) method with a temperature bath of 310 K. The system was maintained at 310 ± 5 K, once heated, by scaling the velocities accordingly (Martyna et al. 1994). Electrostatic interactions were evaluated using the particle mesh ewald (PME) method (Darden et al. 1993). The atom-based non-bonded interactions were truncated beyond 9 Å using a force shift approach. The non-bonded lists were maintained for pairs within a distance of 10 Å and updated heuristically whenever an atom had moved more than 1 Å since last update. Coordinates were saved every 1 ps for further analyses.

The initial confirmations for 2-AG in POPC bilayer were constructed by placing the minimized solute (1-AG and 2-AG) into pre-equilibrated POPC bilayer (approximate 75 POPC each layer, and 11,270 waters) according to the hypothesis therein. The steric overlap between the initial placed solute and lipid/water molecules was relieved by allowing the latter to adiabatically relax in the presence of the solute. The modeling system was first equilibrated for 5,000 steps of steepest descent and 5,000 steps of conjugate gradient minimization, while holding the solute heavy atoms restrained to their initial positions by means of a harmonic force constant 50 kcal/mol/Å$^2$. Then, while maintaining the positional restraints on the solute, the solvent was heated to 310 K in a 600 ps MD phase using a constant pressure of 1 atm. The system was then equilibrated for 1,000 ps followed by an unrestrained simulation at a constant temperature of 310 K and a constant pressure of 1 atm. for 10 ns. The simulations were stable after 6 ns.

## Results

As shown in Fig. 2, four equivalent $^2$H labels were placed on the glycerol backbone of the 2-AG molecule. REDOR NMR spectra were collected ($^2$H observe, $^{31}$P dephasing), for different "dephasing duration times" $\tau$ (from 1.8 to 12 ms). The signal without dephasing ($S_0$) and the signal with dephasing ($S$) were measured by integrating the spectra as displayed in Table 1. Figure 3a shows the experimental signal $S_0$ and $S$, and Fig. 3b shows the ratio of $S/S_0$ against dephasing time, $\tau$. The ratio $S/S_0$ was calculated according to multiple dipole interaction theory with Eq. 2. The dipolar coupling constant is inversely proportional to the cube of the inter-nuclear distance ($1/r^3$). To determine the distance from each deuteron to the phosphorus, the POPC headgroup is arranged in a hexagonal array, as shown in Fig. 4. The four phosphorus atoms $P_1$, $P_2$, $P_3$, and $P_4$ form a parallelogram, each side $b = 8.8$ Å and internal angles of 60° and 120°. Assuming 2-AG intercalates between the lipid molecules, we modeled the average location of the $^2$H labels as a distance $z$ directly above or below the center of the parallelogram. For different $z$ values (shown in Table 2), the $^2$H–$^{31}$P inter-nuclear distances were calculated for $0 \leq \tau \leq 12$ ms and the results displayed in Table 3. The fittings are displayed in Fig. 5 for $z = 0$, 1, and 2 Å, respectively. Each result involved calculation and summation of 893,101 terms. Based on the three curve fittings shown (Fig. 5), the square sums of the difference are 0.193, 0.314, and 0.482 for $z = 0$, 1, and 2 Å, respectively. Clearly, the calculations with $z = 0$ (Fig. 5a) five fits the data the best, which means these methylene $^2$H atoms are at the same level as the phosphate group of the POPC lipid bilayer. The average location of these $^2$H atoms is surrounded by four phosphorus atoms, with two $^{31}$P atoms each 7.6 Å from the average $^2$H location and two other $^{31}$P atoms each 4.4 Å from the average $^2$H location.

**Table 1** Experimental results for $^2$H–$^{31}$P REDOR for different dephasing times

| Dephasing duration time $\tau$ (ms) | Signal with dephasing $S$ | Signal without dephasing $S_0$ | Ratio $\frac{S}{S_0}$ |
|---|---|---|---|
| 1.8 | 1.32E+08 | 1.33E+08 | 0.991 |
| 3.6 | 8.87E+07 | 1.06E+08 | 0.834 |
| 6.0 | 2.54E+07 | 6.83E+07 | 0.372 |
| 7.2 | 3.20E+07 | 8.77E+07 | 0.365 |
| 7.8 | 1.83E+07 | 4.40E+07 | 0.417 |
| 9.0 | 4.54E+07 | 7.03E+07 | 0.646 |
| 9.6 | 1.70E+07 | 4.64E+07 | 0.367 |
| 10.2 | 4.21E+07 | 7.00E+07 | 0.601 |
| 10.8 | 2.61E+07 | 4.08E+07 | 0.640 |
| 11.4 | 2.30E+07 | 4.16E+07 | 0.554 |
| 12.0 | 2.68E+07 | 5.49E+07 | 0.488 |

Molecular dynamic simulations were used to investigate the interaction and orientation of the headgroup of 2-AG in the POPC phospholipid bilayers. Simulations 6 and 10 ns were conducted in pre-equilibrated POPC bilayer. Figure 6 shows the position of 2-AG (CPK with green carbon) simulations in the POPC bilayer at 6 and 10 ns. The insert at the bottom right corner of each graph shows the detailed

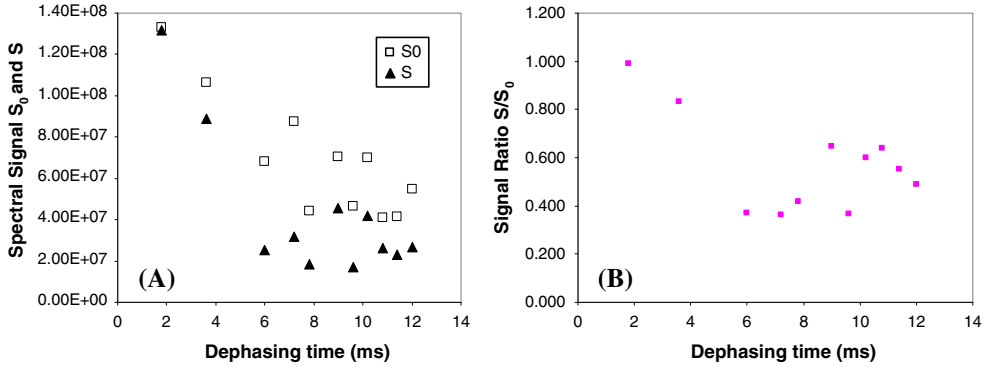


**Fig. 3** **a** Experimental REDOR signals $S_0$ (*open squares*) and $S$ (*close triangles*). **b** The ratio $S/S_0$

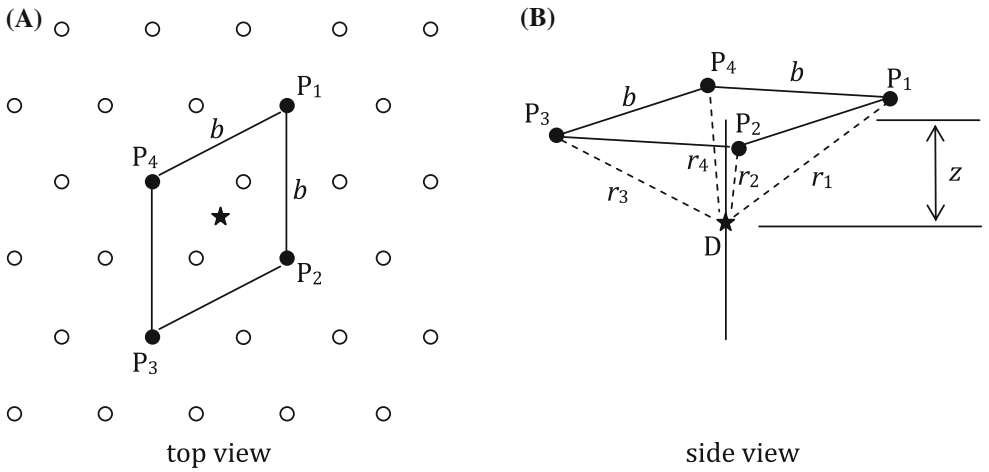


**Fig. 4** **a** The *dark circles* in the *top view* represents $^{31}$P nuclei surrounded by the average location of the four $^{2}$H labels, (*the star*). The *side view* represents distance from each phosphorus to the average location of the four $^{2}$H labels

**Table 2** The $z$ value was adjusted, and $S/S_0$ was calculated for $0 \leq \tau \leq 12$ ms

| $\tau$ (ms) | $S/S_0$ | | |
|---|---|---|---|
| | $z = 0$ | $z = \pm 1$ Å | $z = \pm 2$ Å |
| 0 | 1.000 | 1.000 | 1.000 |
| 1 | 0.983 | 0.985 | 0.990 |
| 2 | 0.935 | 0.944 | 0.961 |
| 3 | 0.863 | 0.879 | 0.915 |
| 4 | 0.775 | 0.798 | 0.855 |
| 5 | 0.684 | 0.709 | 0.783 |
| 6 | 0.600 | 0.621 | 0.703 |
| 7 | 0.532 | 0.541 | 0.621 |
| 8 | 0.484 | 0.474 | 0.538 |
| 9 | 0.458 | 0.423 | 0.459 |
| 10 | 0.451 | 0.389 | 0.387 |
| 11 | 0.458 | 0.370 | 0.323 |
| 12 | 0.473 | 0.362 | 0.269 |

**Table 3** Inter-nuclear distances

| $z$ (Å) | Distance $DP_1$ or $DP_3$ (Å) $r_1 = r_3 = \sqrt{z^2 + (b\cos 30^\circ)^2}$ | Distance $DP_2$ or $DP_4$ (Å) $r_2 = r_4 = \sqrt{z^2 + (b\sin 30^\circ)^2}$ |
|---|---|---|
| 0 | 7.6 | 4.4 |
| 1 | 7.7 | 4.5 |
| 2 | 7.9 | 4.8 |
| 3 | 8.2 | 5.3 |
| 4 | 8.6 | 5.9 |
| 5 | 9.1 | 6.7 |

orientation of 2-AG as well as the hydrogen-bonding interactions in that particular snapshot. After 6-ns simulation, the pattern of H-bonding in 2-AG involves the interactions of the C=O on the arachidonic acid, as well as the two hydroxyl groups at the C1 and C2 sites of the glycerol backbone with $PO_4$ on the POPC headgroup/water

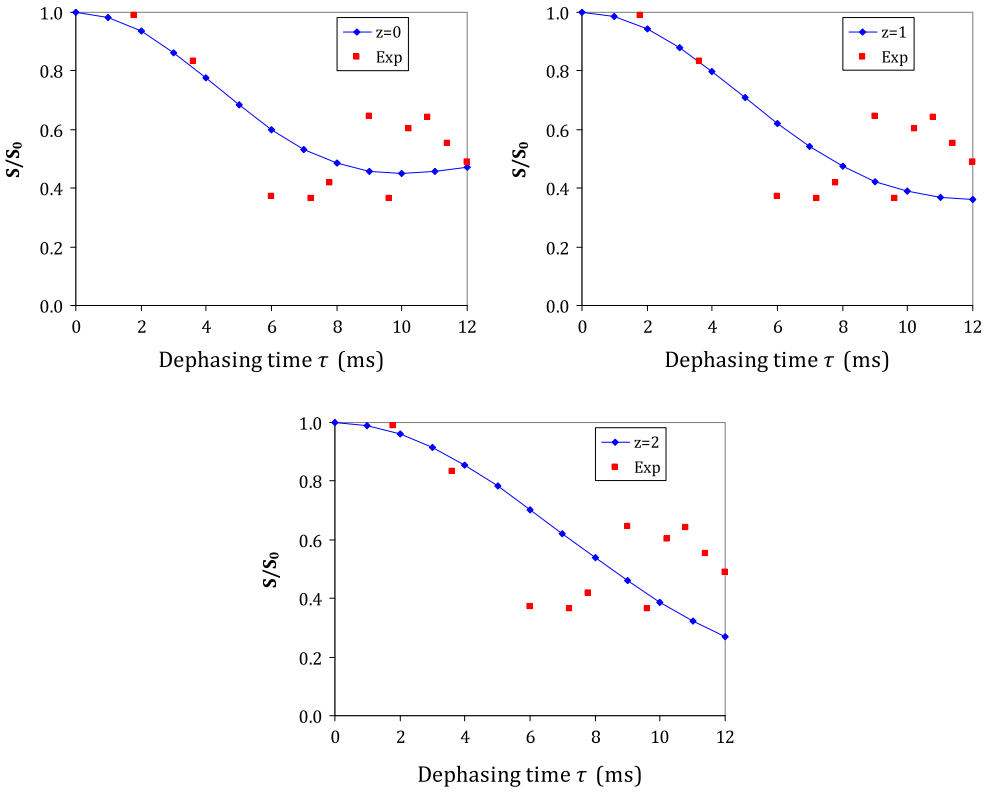


**Fig. 5** Calculated $S/S_0$ for ($z = 0$), ($z = \pm 1$ Å), and ($z = \pm 2$ Å) compared with experimental data. Each result involved calculation and summation of 893,101 terms

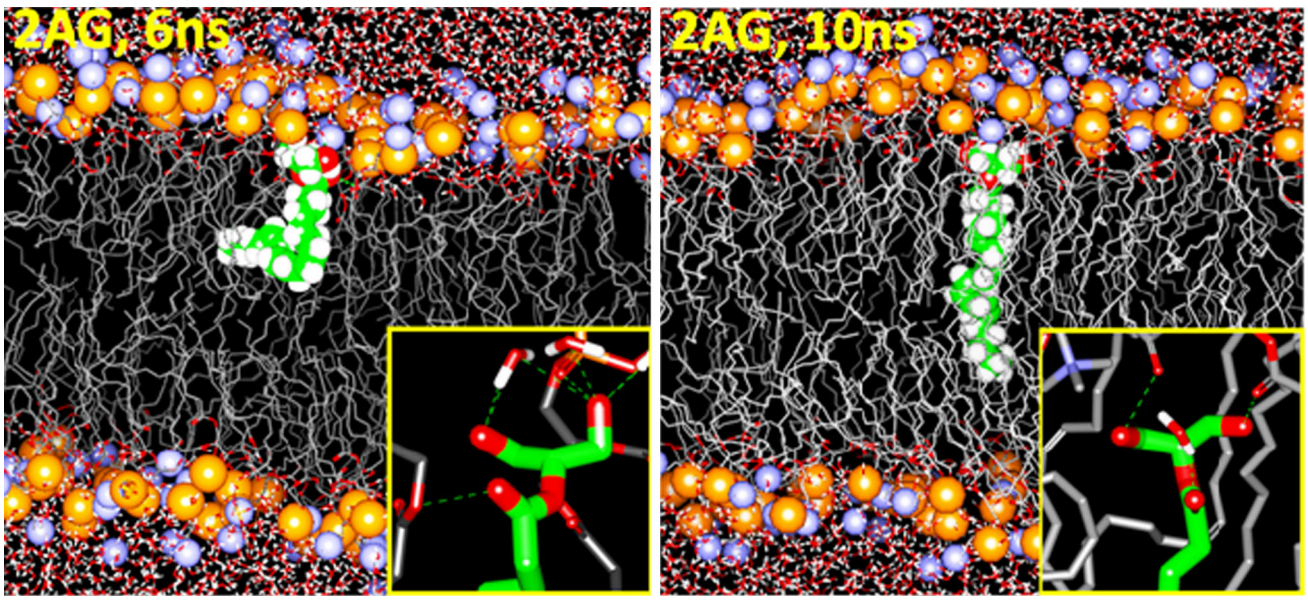


**Fig. 6** Molecular dynamic simulation of 2-AG simulations (CPK with green carbon) in the POPC phospholipid bilayer after 6 and 10 ns. The *inset* at the *bottom right corner* of each graph shows the detailed orientation of 2-AG at that particular snapshot

interface. Essentially, this interaction prototype is maintained after 10-ns simulation except that the headgroup of 2-AG creates a triangle-shaped H-bond network that stabilizes the 2-AG headgroup at the lipid/water interface. Note that, the hydrophobic tail of the neurolipid is extended after 10 ns of simulation.

## Discussion

The glyceryl ester of arachidonic acid (2-AG) has been well known as an important endogenous cannabinoid receptors ligand, but its mode of action is yet to be deduced (Piomelli 2003; Di Marzo 2008; Dinh et al. 2002; Pike et al. 2002). 2-AG is a long fatty acid with four double bonds in carbon positions 5, 8, 11, and 14 and is attached to carbon position 2 of glycerol. It is speculated that 2-AG may exhibit its cannabinergic potency toward the cannabinoid receptors by diffusion through the membrane environment. In these studies, it is demonstrated that within the membrane environment, the arachidonic acid acyl chain is parallel to the phospholipid long molecular axis, and the glycerol backbone region of the ligand is interacting with the lipid headgroup. The conformational dynamics of the ligand, based on the REDOR studies provided evidence that with $z = 0$, the methylene $^{2}$H atoms of 2-AG are at the same level as the phosphate group of the POPC lipid. The average location of the $^{2}$H atoms are surrounded by four phosphorus atoms, with two $^{31}$P atoms each 7.6 Å from the average $^{2}$H location and two other $^{31}$P atoms each 4.4 Å from the average $^{2}$H location. Though $S_0$ or $S$ should exhibit a smooth exponential decay as $\tau$ increases, both the experimental $S$ and $S_0$ have a significant distortion showing the data are good for $\tau < 6$ ms. This means the interactions are stronger for shorter dephasing times. However, the data become a little diffuse for $\tau > 6$ ms perhaps due to noise or background in the spectra caused by weaker interactions of the nuclei pair. This observation may be attributed to multiple spin–spin interactions between 5 $^{2}$H on 2-AG coupling to $^{31}$P on POPC. Nevertheless, the data points generated from these studies were sufficient to provide the distance reported in this paper.

The current results provide evidence that anchoring of 2-AG headgroup to POPC headgroup/water interface and its long tail sweeping laterally within the hydrophobic core of the membrane may be interesting findings to explain the modulation of the physiochemical properties of the lipid bilayers. These observations might be similar to the action of antimicrobial peptides such as MSI-78 that induce significant changes in the lipid bilayer structure, particularly at high peptide concentrations as revealed by NMR studies (Hallock et al. 2003). Thus, the mechanism of action of antimicrobial peptides may help explain 2-AG/POPC interactions (Henzler Wildman et al. 2003). Nonetheless, the sequence of events may affect receptor structure through membrane/ligand interactions, receptor/membrane interactions, or through a combination of complex interactions that can lead to receptor activation. The structure of 2-AG in the membrane as demonstrated by the current findings is controlled by H-bonding network and the orientation of the headgroup within the membrane setting. These peptides are known to stabilize POPC. These findings support studies involving 2-AG, which implicate its structure to selectivity toward the cannabinoid receptors. Membrane stabilization of 2-AG can also be explained through these interaction schemes as solvent effects impede the free circulation of 2-AG and the ability of the ligand to be easily converted to 1-AG. To confirm whether membrane stabilization of 2-AG occurs through H-bonding network between the ligand and POPC, the ligand was allowed to sit in POPC environments at one hand and in dimethyl sulfoxide for protracted length of time. Upon analysis of the components within the two environments using 1-D NMR techniques, the liability of the ligand conversion from 2-AG to 1-AG was only an issue with the organic solvents but not in POPC membrane environment (data not shown). These findings, therefore, set the stage for developing membrane mimetic environment to incorporate 2-AG for future biological studies instead of using simple organic solvents that can complicate the interpretation of assay results.

In conclusion, conformational dynamics in 2-AG is a requirement for cannabinoid receptors activation. The mechanism involves the stabilization of the neurolipid headgroup by the polar headgroup of the membrane environment, thereby causing the long hydrophobic tail to sweep laterally across the membrane, an event which is critical for receptor activation. These results will provide a template for further development of new ligands against the cannabinoid receptors.

**Acknowledgments** This study was supported by the National Institutes of Health on Drug Abuse Grant No. RDA027849A (EKT).

## References

Bowers KJ, Chow E, Xu H, Dror RO, Eastwood MP, Gregersen BA, Klepeis JL, Kolossváry I, Moraes MA, Sacerdoti FD, Salmon JK, Shan Y, Shaw DE (2006) Scalable algorithms for molecular dynamics simulations on commodity clusters. In Proceedings of the ACM/IEEE conference on supercomputing (SC06). Tampa, FL

Cravatt BF, Giang DK, Mayfield SP, Boger DL, Lerner RA, Gilula NB (1996) Molecular characterization of an enzyme that degrades neuromodulatory fatty-acid amides. Nature 384:83–87

Darden T, York D, Pedersen LG (1993) Particle mesh Ewald: an N log(N) method for Ewald sums in large systems. J Chem Phys 98:10089–10095

De Angelis AA, Opella SJ (2007) Bicelle samples for solid-state NMR of membrane proteins. Nat Protoc 2:2332–2338

Devane WA, Hanus L, Breuer A, Pertwee RG, Stevenson LA, Griffin G, Gibson D, Mandelbaum A, Etinger A, Mechoulam R (1992) Isolation and structure of a brain constituent that binds to the cannabinoid receptor. Science 258:1946–1949

Di Marzo V (2008) Targeting the endocannabinoid system: to enhance or reduce? Nat Rev Drug Discov 7:438–455

Dinh TP, Freund TF, Piomelli D (2002) A role for monoglyceride lipase in 2-arachidonoylglycerol inactivation. Chem Phys Lipids 121:149–158

Goetz JM, Schaefer J (1997) REDOR dephasing by multiple spins in the presence of molecular motion. J Magn Reson 127:147–154

Grage SL, Watts JA, Watts A (2004) 2H[19F] REDOR for distance measurements in biological solids using a double resonance spectrometer. J Magn Reson 166:1–10

Guo J, Pavlopoulos S, Tian X, Lu D, Nikas SP, Yang DP, Makriyannis A (2003) Conformational study of lipophilic ligands in phospholipid model membrane systems by solution NMR. J Med Chem 46:4838–4846

Hallock KJ, Lee DK, Ramamoorthy A (2003) MSI-78, an analogue of the magainin antimicrobial peptides, disrupts lipid bilayer structure via positive curvature strain. Biophys J 84:3052–3060

Henzler Wildman KA, Lee DK, Ramamoorthy A (2003) Mechanism of lipid bilayer disruption by the human antimicrobial peptide, LL-37. Biochemistry 42:6545–6558

Hurst DP, Grossfield A, Lynch DL, Feller S, Romo TD, Gawrisch K, Pitman MC, Reggio PH (2010) A lipid pathway for ligand binding is necessary for a cannabinoid G protein-coupled receptor. J Biol Chem 285:17954–17964

Jorgensen WL, Maxwell DS, Tirado-Rives J (1996) Development and testing of the OPLS all-atom force field on conformational energetics and properties of organic liquids. J Am Chem Soc 118:11225–11236

Kozak KR, Prusakiewicz JJ, Marnett LJ (2004) Oxidative metabolism of endocannabinoids by COX-2. Curr Pharm Des 10:659–667

Kräutler V, van Gunsteren WF, Hünenberger PH (2001) A fast SHAKE algorithm to solve distance constraint equations for small molecules in molecular dynamics simulations. J Comput Chem 22:501–508

Lynch DL, Reggio PH (2005) Molecular dynamics simulations of the endocannabinoid N-arachidonoylethanolamine (anandamide) in a phospholipid bilayer: probing structure and dynamics. J Med Chem 48:4824–4833

Makriyannis A, Yang DP, Griffin RG, Das Gupta SK (1990) The perturbation of model membranes by (-)-delta 9-tetrahydrocannabinol. Studies using solid-state 2H- and 13C-NMR. Biochim Biophys Acta 1028:31–42

Martyna GJ, Tobias DJ, Klein ML (1994) Constant pressure molecular dynamics algorithms. J Chem Phys 101:4177–4189

Matsuda LA, Lolait SJ, Brownstein MJ, Young AC, Bonner TI (1990) Structure of a cannabinoid receptor and functional expression of the cloned cDNA. Nature 346:561–564

Mavromoustakos T, Daliani I (1999) Effects of cannabinoids in membrane bilayers containing cholesterol. Biochim Biophys Acta 1420:252–265

Mechoulam R, Ben-Shabat S, Hanus L, Ligumsky M, Kaminski NE, Schatz AR, Gopher A, Almog S, Martin BR, Compton DR et al (1995) Identification of an endogenous 2-monoglyceride, present in canine gut, that binds to cannabinoid receptors. Biochem Pharmacol 50:83–90

Murillo-Rodriguez E, Blanco-Centurion C, Sanchez C, Piomelli D, Shiromani PJ (2003) Anandamide enhances extracellular levels of adenosine and induces sleep: an in vivo microdialysis study. Sleep 26:943–947

Pike LJ, Han X, Chung KN, Gross RW (2002) Lipid rafts are enriched in arachidonic acid and plasmenylethanolamine and their composition is independent of caveolin-1 expression: a quantitative electrospray ionization/mass spectrometric analysis. Biochemistry 41:2075–2088

Piomelli D (2003) The molecular logic of endocannabinoid signalling. Nat Rev Neurosci 4:873–884

Raghunathan VA, Katsaras J (1995) Structure of the Lc' phase in a hydrated lipid multilamellar system. Phys Rev Lett 74:4456–4459

Reggio PH (2010) Endocannabinoid binding to the cannabinoid receptors: what is known and what remains unknown. Curr Med Chem 17:1468–1486

Sugiura T, Kondo S, Sukagawa A, Nakane S, Shinoda A, Itoh K, Yamashita A, Waku K (1995) 2-Arachidonoylglycerol: a possible endogenous cannabinoid receptor ligand in brain. Biochem Biophys Res Commun 215:89–97

Szabo B, Urbanski MJ, Bisogno T, Di Marzo V, Mendiguren A, Baer WU, Freiman I (2006) Depolarization-induced retrograde synaptic inhibition in the mouse cerebellar cortex is mediated by 2-arachidonoylglycerol. J Physiol 577:263–280

Tian X, Guo J, Yao F, Yang DP, Makriyannis A (2005) The conformation, location, and dynamic properties of the endocannabinoid ligand anandamide in a membrane bilayer. J Biol Chem 280:29788–29795

Tiburu EK, Dave PC, Lorigan GA (2004) Solid-state 2H NMR studies of the effects of cholesterol on the acyl chain dynamics of magnetically aligned phospholipid bilayers. Magn Reson Chem 42:132–138

Tiburu EK, Bass CE, Struppe JO, Lorigan GA, Avraham S, Avraham HK (2007) Structural divergence among cannabinoids influences membrane dynamics: a 2H solid-state NMR analysis. Biochim Biophys Acta 1768:2049–2059

Tuckerman ME, Berne BJ, Rossi A (1991) Molecular dynamics algorithm for multiple time scales: systems with disparate masses. J Chem Phys 101:1465–1471

Yang DP, Mavromoustakos T, Beshah K, Makriyannis A (1992) Amphipathic interactions of cannabinoids with membranes. A comparison between delta 8-THC and its O-methyl analog using differential scanning calorimetry, X-ray diffraction and solid state 2H-NMR. Biochim Biophys Acta 1103:25–36